Received: 30 April 2020 | Revised: 14 July 2020 | Accepted: 23 January 2021

DOI: 10.1002/hipo.23311

RESEARCH ARTICLE

WILEY

Hippocampal beta oscillations predict mouse object-location associative memory performance

Satoshi Iwasaki[1] | Takuya Sasaki[1,2] | Yuji Ikegaya[1,3]

[1]Graduate School of Pharmaceutical Sciences, The University of Tokyo, Tokyo, Japan

[2]Precursory Research for Embryonic Science and Technology (PRESTO), Japan Science and Technology Agency (JST), Saitama, Japan

[3]Center for Information and Neural Networks, National Institute of Information and Communications Technology, Suita City, Osaka, Japan

Correspondence
Yuji Ikegaya, Laboratory of Chemical Pharmacology Graduate School of Pharmaceutical Sciences, The University of Tokyo 7-3-1 Hongo, Bunkyo-ku, Tokyo 113-0033, Japan.
Email: yuji@ikegaya.jp

Funding information
JSPS Grants-in-Aid for Scientific Research, Grant/Award Number: 18H05525; JST ERATO, Grant/Award Number: JPMJER1801; the AMED Strategic International Brain Science Research Promotion Program, Grant/Award Number: 18dm0307007h0001; the Human Frontier Science Program, Grant/Award Number: RGP0019/2016

Abstract

Memorizing the locations of environmental cues is crucial for survival and depends on the hippocampus. We recorded local field potentials (LFPs) from the hippocampus of freely moving mice during an object location task. The power of beta-band (23–30 Hz) oscillations increased immediately before approaching objects in a memory-encoding phase. The exploration-induced beta oscillations gradually decreased during the memory-encoding session. Mice that exhibited stronger beta oscillation power exhibited better performance in the subsequent memory-retrieval test. These results suggest that beta oscillations in the hippocampal CA1 region are involved in the memory encoding of object-location associations.

KEYWORDS
hippocampus, local field potential, slow gamma, object location memory

1 | INTRODUCTION

Memories about the locations of environmental cues underlie spatial navigation or episodic memories. Out of three main components in episodic memories, that is, "what," "where," and "when" (Tulving, 1983), the first two components can be experimentally assessed using the object location task in rodents (Ennaceur, Neave, & Aggleton, 1997; Vogel-Ciernia & Wood, 2014). In this task, an animal is placed in an arena equipped with two identical objects and is subsequently reexposed to the same arena after one of the objects had been moved to another location. Because of the nature of neophilia, the animal explores the relocated object more when it remembers the previous locations of the objects. The object location task has been widely used in pharmacological and psychological tests because it relies only on spontaneous exploratory behaviors of animals and does not need any reinforcement or punishment. Object location memories are impaired by pharmacological inactivation or surgical lesions of the hippocampus (Assini, Duzzioni, & Takahashi, 2009; Barker & Warburton, 2011) and are modulated by glutamatergic *N*-methyl-D-aspartate (NMDA) receptors and cholinergic muscarinic receptors (Assini et al., 2009; Murai, Okuda, Tanaka, & Ohta, 2007). Nonetheless, the hippocampal circuit mechanisms for object location memories remain unclear.

Accumulating evidence shows that the hippocampus exhibits characteristic neuronal oscillations, that is, local field potentials (LFPs) that reflect the ensemble activity of neurons (Buzsáki & Draguhn, 2004; Buzsáki & Wang, 2012). Numerous studies have elucidated the behavioral correlates of hippocampal 6–9 Hz (theta) oscillations (Buzsáki, 2002; Colgin, 2013), 60–90 Hz (gamma) oscillations (Buzsáki & Wang, 2012), and 150–250 Hz (ripple) oscillations (Buzsáki, 2015; Girardeau, Benchenane, Wiener, Buzsáki, & Zugaro, 2009; Norimoto et al., 2018) to memory processes, and less attention has been paid to beta (23–30 Hz) oscillations, which have been implicated in novelty detection. When mice were exposed to a

novel track, hippocampal 23–30 Hz power increased after the first lap and was subsequently attenuated within a few minutes (Berke, Hetrick, Breck, & Greene, 2008). Another study demonstrated that hippocampal 23–30 Hz power was enhanced during novel object exploration and reduced over the course of the session and that 23–30 Hz power was low when the mice were reexposed to the objects (França et al., 2014). These reports suggested that novel experiences induced an increase in hippocampal 23–30 Hz power and may establish a brain state that is prepared for learning. However, previous studies have lacked detailed characteristics about hippocampal 23–30 Hz oscillations; for example, these studies analyzed only the overall changes in the 23–30 Hz oscillations, but the exact behavioral correlates to the 23–30 Hz oscillations were not identified.

In the present study, we monitored hippocampal LFPs in freely moving mice during the object location task and found that a transient increase in hippocampal 23–30 Hz oscillations occurred immediately before each exploratory behavior toward an object. Moreover, mice that exhibited greater increases in 23–30 Hz power during memory encoding exhibited better memory recall. These correlations are consistent with the possibility that hippocampal 23–30 Hz oscillations promote learning about the locations of environmental cues.

2 | METHODS

2.1 | Animals

This study was conducted in accordance with the NIH guidelines for the care and use of animals. The protocol was approved by the Experimental Animal Ethics Committee of the University of Tokyo (approval number: P29-14). Adult male C57BL/6J mice (SLC, Shizuoka, Japan), 7–11 weeks old, were housed under conditions of controlled temperature and humidity (23 ± 1°C, 55 ± 5%), maintained on a 12:12 hr light/dark cycle, and had access to ad libitum food and water. A total of eight mice were used for the recordings. The mice were individually housed after surgery. The mice were acclimated to the experimental environments via daily handling before behavioral experiments.

2.2 | Behavioral procedure

The object location task was conducted in an open-topped square container that measured 30 × 30 × 27 cm^3 and had a smooth floor and several visual cue cards on the wall. Before the task, mice were habituated to this open arena for 10 min on 2 consecutive days. During the encoding phase, one mouse was placed in the arena that was equipped with two novel identical objects in separate corners and was allowed to freely explore them and the arena for 10 min. Thirty minutes after the encoding phase, one of the objects was moved to another corner, and the mouse was allowed to explore the arena and objects for 5 min. The task was performed between 6:00 p.m. and 11:00 p.m. The same mice were repeatedly tested up to five times using different novel objects at intervals of more than 2 days. The arena and objects were cleaned with 70% ethanol before each trial. In the experiments in Figure 1, the mice were intraperitoneally administered 5 mg/kg clozapine-*N*-oxide (CNO; ab141704, Abcam, Cambridge, UK) or saline 30 min before the encoding phase ("CNO group" or "Saline group," respectively). These mice were assigned into the Saline group and the CNO group and used in a crossover design. For each session, a discrimination index was calculated as $T_D/(T_N + T_D)$, where T_N and T_D represent the

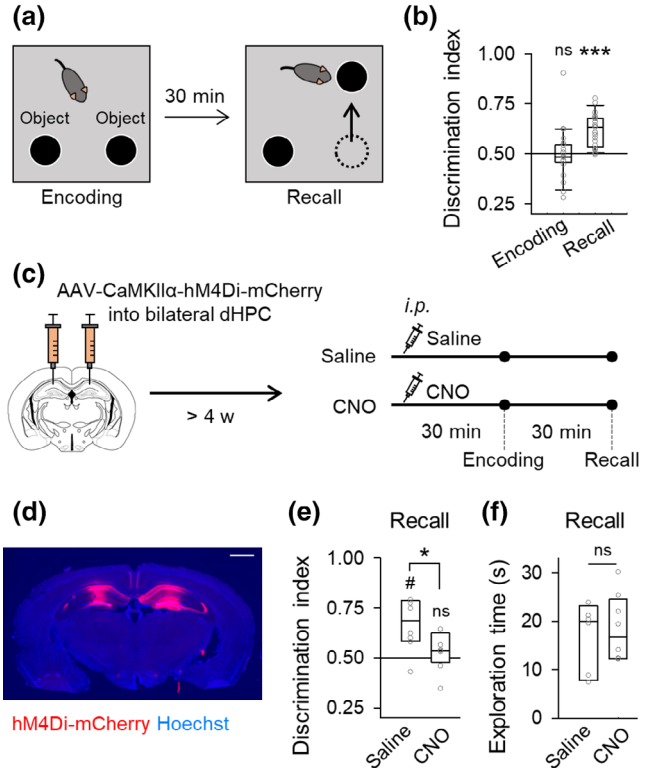

FIGURE 1 The object location task depends on the hippocampus. (a) Experimental scheme of the object location task. Thirty minutes after a mouse was allowed to explore a field with two novel identical objects for 10 min (*left*, "Encoding"), one of the objects was displaced to a new position, and the mouse was allowed to explore the objects for 5 min (*right*, "Recall"). (b) The discrimination index was calculated based on the times spent exploring the two objects. Mice preferentially explored the displaced objects in the recall phase. ***$p < .001$, one-sample *t* test versus the chance level of .5, $n = 21$ sessions each. (c) Experimental schedule of the object location task with chemogenetic inhibition of hippocampal neuronal activity. Naïve mice that had been injected with AAVs were tested in the object location task. They were intraperitoneally administered saline or CNO 30 min before the encoding phase. (d) Representative image showing hM4Di-mCherry expression in a coronal section that was counterstained with Hoechst. Scale bar, 1 mm. (e) Discrimination indices in the recall phase of AAV-injected subjects. CNO treatment before the encoding phase impaired the object location test performance. *$p < .05$, Student's *t* test, #$p < .05$, one-sample *t* test versus the chance level of .5, $n = 7$ sessions. (f) Total time spent exploring the objects in the recall phase. CNO treatment did not affect exploratory behavior. Student's *t* test, $n = 7$ sessions [Color figure can be viewed at wileyonlinelibrary.com]

times spent exploring the nondisplaced object and the displaced object, respectively.

The behaviors of the mice were monitored at a video frame rate of 15 Hz using a top-view digital camera. Exploratory activity was manually categorized in each frame. A period during which the mouse approached the objects to within 1 cm from its nose with its head being directed toward the objects or touched the object with the nose or forepaws was defined as an exploration event. The following events were excluded from the analysis: (a) the mouse passed by the objects, (b) it climbed on the objects, (c) it groomed itself near the objects, and (d) it approached at instantaneous velocities less than 5 cm/s. To calculate velocity, the video rate was downsampled to 3 Hz, and the instantaneous velocity of each frame was calculated based on the distance traveled during a one-frame period of 333 ms.

2.3 | Surgery

Under anesthesia with isoflurane gas (1–3%), a craniotomy was performed using a high-speed drill, and the dura was surgically removed. An electrode assembly that contained six independently movable tetrodes was created using a 3D printer (Form 2, Formlabs, Somerville, MA) and was stereotaxically implanted above the dorsal hippocampal CA1 region (1.9 mm posterior and 1.70 mm lateral to bregma) and the retrosplenial cortex (2.5 mm posterior and 0.30 mm lateral to bregma) at an angle of 80° relative to the brain surface. The tetrodes were made of 17-μm-wide polyimide-coated platinum-iridium (90/10%) wires (California Fine Wire Co., Grover Beach, CA), and the electrode tips were plated with platinum to have low electrode impedances of 150–300 kΩ. The electrodes were connected to an electrical interface board (Neuralynx, Bozeman, MT) on the microdrive. An incision was made on the neck, and an electromyography electrode wire (AS 633, Cooner Wire Co., Los Angeles, CA) was sutured to the dorsal neck muscles. The ground/reference electrodes were located on the cerebellum. The recording device was secured to the skull using dental cement (Re-fine Bright, Yamahachi Dental Mfg. Co., Aichi, Japan). After all surgical procedures were completed, anesthesia was discontinued, and the mice were allowed to spontaneously awaken. Each animal was housed in a transparent Plexiglas cage with free access to water and food. In the experiments shown in Figure 1 (virus microinjection), AAV_{DJ}-CaMKIIα-hM4Di-mCherry (0.3–0.5 μl, $2–3 \times 10^{13}$ vg/ml) was bilaterally injected into the dorsal hippocampus (1.9 mm posterior, 1.6 mm lateral and 1.4 mm ventral to bregma) at a rate of 0.1 μl/min using glass pipettes.

2.4 | Electrophysiological recording

LFP signals were digitally recorded at a sampling rate of 2 kHz and were low-pass filtered at 500 Hz using a Cereplex direct recording system (Blackrock Microsystems, Salt Lake City, UT). Following the implant surgery, the electrodes were advanced to the targeted brain regions at least 1 week after surgery as previously described (Norimoto et al., 2018; Okada, Igata, Sasaki, & Ikegaya, 2017). Briefly, the depth of the electrode tips was adjusted according to LFP signals recorded while the mouse rested in the home cage. Based on multiunit spiking activity and sharp-wave ripples during periods of immobility, the electrodes above the hippocampus were lowered toward the CA1 pyramidal cell layer. The tetrodes then remained in the targeted area so that stable recordings were obtained over a period of several days. On the recording day, the mouse performed the object location task, and electrical signals were continuously recorded throughout the task and during the 30-min rest periods in the home cage before and after the task.

2.5 | Histological analysis

The mice were overdosed with urethane and α-chloralose and were intracardially perfused with 4% paraformaldehyde in phosphate-buffered saline. The brain samples were postfixed with 4% paraformaldehyde and were subsequently equilibrated with 30% sucrose in phosphate-buffered saline. Frozen coronal sections (40 μm in thickness) that included the hippocampus, were cut using a cryostat, and serial sections were mounted onto slides. The preparations were rinsed in water and stained with cresyl violet. The positions of the recording electrodes were confirmed by identifying the corresponding electrode tracks in histological tissue. We failed to determine electrode positions in one mouse. To verify viral expression, frozen coronal sections were counterstained with Hoechst.

2.6 | LFP analysis

To compute the time-frequency representation of the LFP power (spectrogram), LFP signals were convolved using complex Morlet wavelet transformation at frequencies ranging from 1 to 100 Hz. The absolute LFP power spectrum was calculated every 0.5 ms and normalized by the mean power recorded in their home cages before the task for each frequency. Exploration-induced changes in LFP power were calculated as the average of the normalized power for the 1-s period prior to the exploration onset. The beta oscillation power during nonexploration periods was calculated as the mean power for a 1-min period that did not include the period ranging from −3 to +2 s relative to each exploration onset. The last frame in which the instantaneous velocity decreased below 5 cm/s before exploration onset was defined as the timepoint indicating the beginning of a run preceding an exploration event. Frames in which the instantaneous velocity reached over and fell under 5 cm/s, exception for the periods in the range from −3 to +2 s relative to exploration onset, were defined as timepoints indicating the beginning of a run and stopping of a run without exploration, respectively. To analyze the phase-amplitude coupling between different bands of LFP oscillations, we obtained a modulation index as described in a previous paper (Tort, Komorowski, Eichenbaum, & Kopell, 2010). The modulation index was defined as the normalized Kullback–Leibler distance of the amplitude distribution

across all phases in a uniform distribution. The phases of LFPs were calculated using the Holbert transform. LFPs recorded during the encoding sessions were used for the analysis.

2.7 | Data analysis

All analyses were performed using custom-made MATLAB 2017a routines (Mathworks, Natick, MA). Data are presented as the mean ± *SEM* unless otherwise specified. The null hypothesis was rejected at the $p < .05$ level.

3 | RESULTS

3.1 | Object location task depends on the hippocampus

We used the object location task to assess the memory of mice. We first examined whether the mice could learn this task while carrying recording microdrives on their heads. For 10 min, the mice were allowed to freely explore an open arena that contained two identical objects placed in separate corners (Figure 1a *left*). Thirty minutes after the 10-min encoding phase, one of the objects was displaced to the other corner, and the mice were allowed to explore the objects for 5 min (Figure 1a *right*). If the mice remembered the previous locations of the two objects, the mice would preferentially explore the displaced object because they are innately neophilic. During this recall phase, the mice spent more time exploring the displaced object than the other object (Figure 1b; Encoding: $t_{20} = 0.124$, $p = .903$, Recall: $t_{20} = 6.40$, $p = 3.03 \times 10^{-6}$, one-sample *t* test versus the chance level of .5; $n = 21$ sessions each). To confirm whether the object recognition task was dependent on the hippocampus, we bilaterally injected AAV_{DJ}-CaMKIIα-hM4Di-mCherry into the dorsal hippocampus (Figure 1c,d). In the Saline group, saline was intraperitoneally injected 30 min before the encoding phase. In the CNO group, CNO was injected 30 min before the encoding phase. The mice in the CNO group exhibited poor performance in the object location task (Figure 1e; Saline versus CNO: $t_{12} = 2.20$, $p = 4.81 \times 10^{-2}$, Student's *t* test; Saline: $t_6 = 3.06$, $p = 2.22 \times 10^{-2}$, CNO: $t_6 = 0.494$, $p = .639$, one-sample *t* test versus the stochastic level of 0.5; $n = 7$ sessions). The total exploration time during the recall phase did not differ between the two groups (Figure 1f; $t_{12} = -3.89 \times 10^{-2}$, $p = .970$, Student's *t* test; $n = 7$ sessions). Thus, neuronal activity in the hippocampus is essential for object location memory.

3.2 | Hippocampal 23–30 Hz oscillation power increases before object exploration

To record LFPs, we implanted tetrodes into the hippocampus using custom-made microdrives. After the experiment, the positions of the electrode tips were verified in Nissl-stained coronal sections (Figure 2). LFPs were recorded in a total of 21 sessions from eight animals. Actions involving approaching either of the objects followed by sniffing or

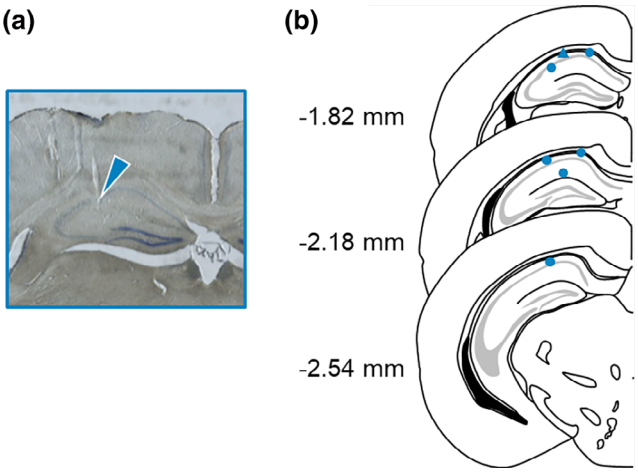

FIGURE 2 Locations of the electrode tips used for recordings. (a) Histological verification of the recording sites. (b) Recording sites in a total of seven mice were pooled in the diagrams. Electrode positions in one mouse were unknown because of reconstruction failure. Circles and triangles indicate the left and right hemispheres, respectively [Color figure can be viewed at wileyonlinelibrary.com]

touching the object were defined as exploration events. Power spectral analyses revealed that in the encoding phase, the oscillation power at frequencies ranging from 23 to 30 Hz increased before the exploration event (Figure 3a,b). This frequency band modulation was consistent with previous studies showing that hippocampal beta oscillations were associated with novelty (Berke et al., 2008; França et al., 2014). The power spectrograms were averaged across all 370 exploration events from 21 sessions (Figure 3c). The increases lasted for ~1 s and disappeared when the exploration event started. The mean 23–30 Hz power during the 1 s before the exploration onset for each mouse was significantly higher than the mean power across the entire session (Figure 3d; $t_7 = 3.63$, $p = 8.41 \times 10^{-2}$, paired *t* test; $n = 8$ mice).

Because associative learning has been reported to induce cross-frequency coupling between theta and low-gamma oscillations in the CA1 (Igarashi, Lu, Colgin, Moser, & Moser, 2014), we analyzed the power-phase interaction during the encoding period. Although the 30–40 Hz amplitude was modulated by the 2–5 Hz phase, no interactions between beta and the other oscillations were detected in the phase-amplitude coupling plot (Figure 3e), suggesting that the observed increase in beta oscillations was generated independently of the other frequency oscillations. Sniffing behavior itself may be associated with hippocampal 10–20 Hz oscillations (Lockmann, Laplagne, & Tort, 2018), but we did not observe an increase in 23–30 Hz oscillations during sniffing without object explorations (Figure 3f). Thus, 23–30 Hz oscillations reflected object exploratory behavior and not sniffing per se.

Exploration-induced increases in the 23–30 Hz power were more evident during the first few minutes of the encoding phase than during the later period (Figure 3g,h; $^{**}p < .01$ versus 0–1 or 4–10 min, Tukey–Kramer post hoc test; $F_{9,360} = 6.19$, $p = 3.92 \times 10^{-8}$, one-way ANOVA; $n = 16$–70 events from 21 sessions). On the other hand, the 23–30 Hz power during nonexploration periods changed only modestly during the encoding phase (Figure 3h). Throughout the sessions,

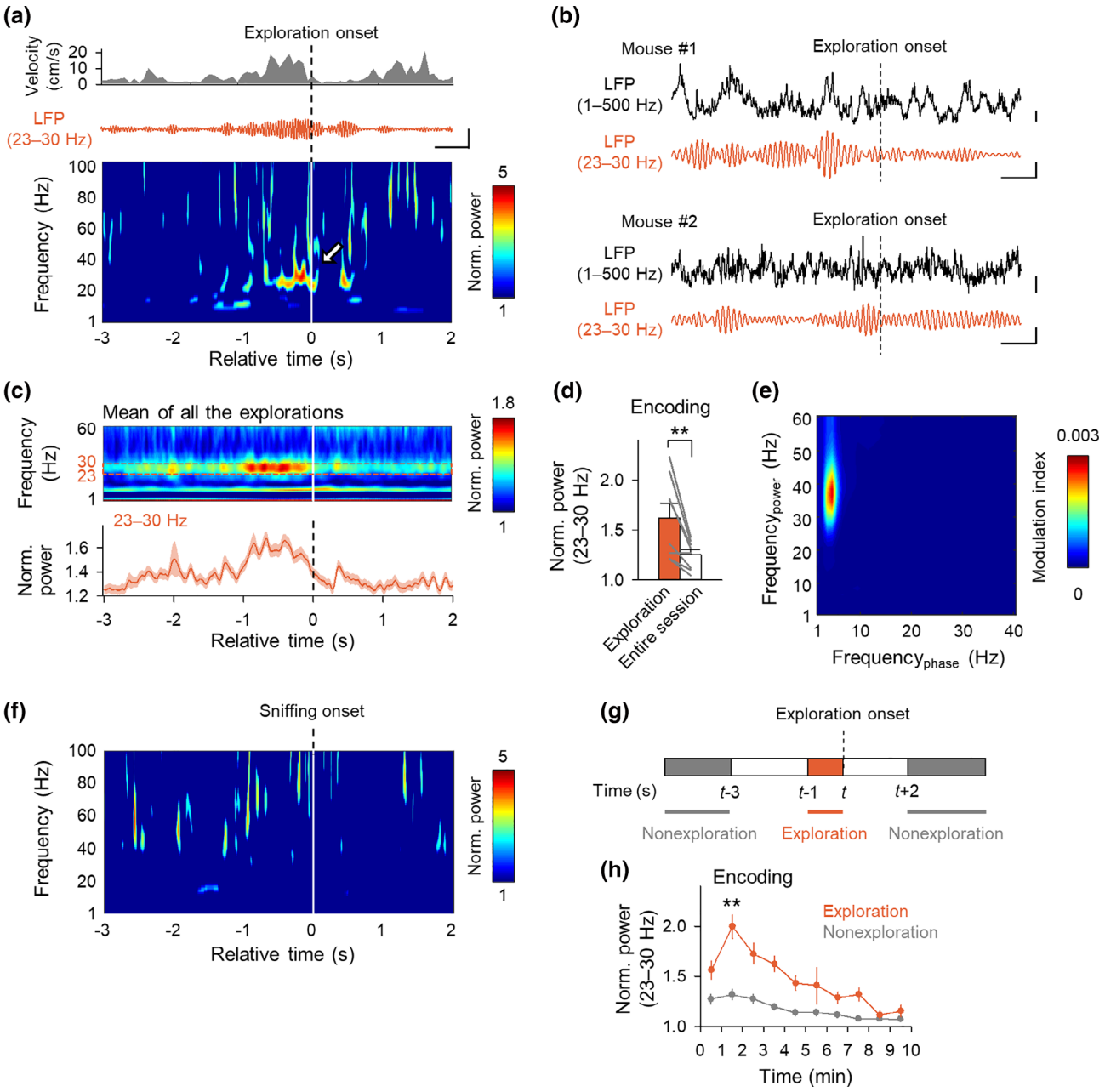

FIGURE 3 Hippocampal 23–30 Hz oscillation power transiently increases before object exploration. (a) Representative time course of exploratory behavior and hippocampal CA1 LFP. *Top*, moving speed of a mouse. The *vertical line* at time 0 indicates the onset of an exploration event. *Middle*, a trace of 23–30 Hz-filtered LFP. Scale: 2 mV (vertical) and 0.5 s (horizontal). *Bottom*, power spectrogram of LFP computed using the wavelet transform, which was normalized for each frequency to the mean LFP power that was recorded in a home cage. The *arrow* indicates an increase in 23–30 Hz oscillations. (b) Example raw traces of exploration-induced 23–30 Hz oscillations. Scale: 2 mV (vertical, 1–500 Hz), 0.5 mV (vertical, 23–30 Hz), and 0.25 s (horizontal). (c) *Top*, mean power spectrograph of hippocampal LFPs from a total of 370 exploration events from 21 sessions. The *vertical line* at time 0 indicates the onset of an exploration event. *Bottom*, Mean ± *SEM* change over time in the 23–30 Hz-filtered LFP power. (d) The means ± *SEM* of the 23–30 Hz power during a 1-s period preceding the exploration onset for each animal was significantly greater than the mean power of the entire session. $^{**}p < .01$, paired *t* test, $n = 8$ mice. (e) Cross-frequency coherence plot averaged for all recorded encoding sessions. (f) Representative power spectrogram of LFPs during sniffing behavior without object exploration. The *vertical line* at time 0 indicates the onset of sniffing behavior toward the wall of the arena. Similar results were observed in all other mice. (g) Definitions of the periods for exploration and nonexploration. Exploration was calculated as the average of the 23–30 Hz power for the 1-s period prior to the exploration onset, whereas nonexploration was calculated as the mean power for a 1-min period without periods ranging from −3 s to +2 s relative to each exploration onset. (h) Time changes in the mean ± *SEM* power during a 1-s period before exploration onset (orange) and during the nonexploration period (gray). $^{**}p = 6.6 \times 10^{-3}$ versus 0–1 min, $Q = 75.6$; $^{**}p < .01$ versus 4–10 min, $F_{9,360} = 6.19$; Tukey–Kramer test after one-way ANOVA; $n = 16$–70 events from 21 sessions [Color figure can be viewed at wileyonlinelibrary.com]

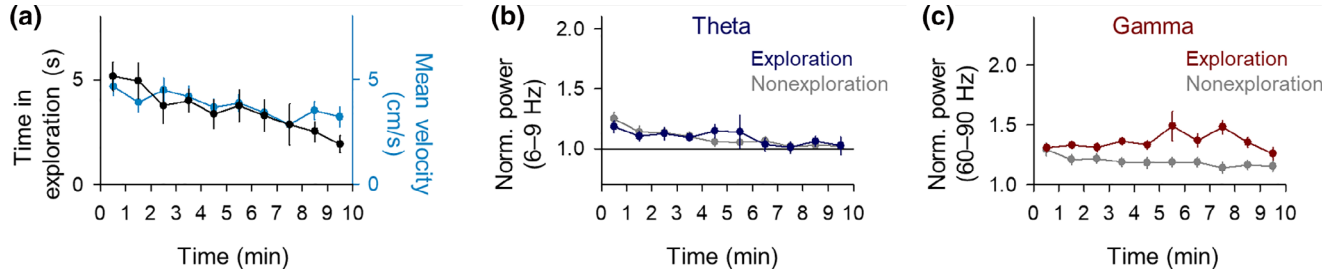

FIGURE 4 Exploratory behavior and theta oscillations gradually decrease during the encoding phase. (a) Temporal changes in time spent exploring (*black*) and mean velocity (*blue*); *n* = 21 sessions. (b and c) Change over time in the mean power of theta (B, 6–9 Hz) and gamma (C, 60–90 Hz) oscillations in a 1-s period before the onset of object exploration; *n* = 21 sessions [Color figure can be viewed at wileyonlinelibrary.com]

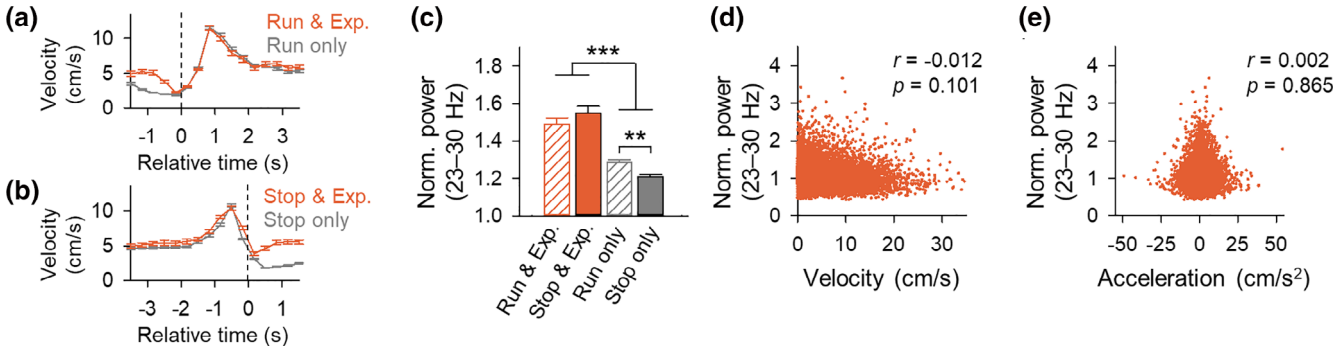

FIGURE 5 Locomotion cannot explain the increase in exploration-induced 23–30 Hz oscillation power. (a) Mean ± *SEM* running speed at the initiation times of running with exploration (*orange*) and without exploration (*gray*); *n* = 363 and 696 running events, respectively, from 21 sessions. (b) Mean ± *SEM* running speed at the times of stopping with exploration (*orange*) and without exploration (*gray*); *n* = 365 and 1,065 stopping events, respectively, from 21 sessions. (c) Mean ± *SEM* 23–30 Hz oscillation power immediately after beginning to run and before stopping. ***$p < .001$, **$p < .01$, Tukey–Kramer test after one-way ANOVA; *n* = 363–1,065 events from 21 sessions. (d) A scatter plot between the 23–30 Hz power and velocity in 1-s windows. $r = -.012$, $p = .10$, Pearson's test. (e) A scatter plot between the 23 and 30 Hz power and acceleration; $r = .002$, $p = .87$, Pearson's test [Color figure can be viewed at wileyonlinelibrary.com]

the time spent exploring and the mean velocity of locomotion gradually decreased during the encoding phase (Figure 4a). The theta (6–9 Hz) or gamma (60–90 Hz) power remained nearly constant across encoding phases (Figure 4b,c; Exploration theta: $F_{9,360} = 0.911$, $p = .518$, one-way ANOVA, *n* = 16–70 events from 21 sessions; Exploration gamma: $F_{9,360} = 1.72$, $p = 8.23 \times 10^{-2}$, one-way ANOVA, *n* = 16–70 events from 21 sessions). These observations suggested that exploration-induced 23–30 Hz oscillations reflect a cognitive process such as attention or curiosity to environmental saliency.

3.3 | Locomotion cannot explain exploration-induced 23–30 Hz power increases

During an exploratory event, mice ran toward the objects and stopped in front of them. Thus, it is possible that these behavioral actions per se enhanced the 23–30 Hz power, irrespective of cognitive processes. We analyzed the 23–30 Hz power when mice began to run or stop with or without object exploration. When mice ran or stopped without a subsequent exploration event, the locomotion speed changed in a similar manner as observed when they explored the objects (Figure 5a,b), but the increases in the 23–30 Hz power without exploration events were smaller than those with exploration events (Figure 5c; ***$p < .001$, **$p < .01$, Tukey–Kramer post hoc test; $F_{3,2,522} = 62.2$, $p = 8.05 \times 10^{-39}$, one-way ANOVA; *n* = 363–1,065 events from 21 sessions). Even during the object exploration, there was no significant correlation between the 23 and 30 Hz power and the instantaneous velocities (Figure 5d; $r = -.012$, $p = .101$, Pearson's test) or acceleration (Figure 5e; $r = .002$, $p = .865$). These results suggested that the increased 23–30 Hz oscillations before the exploration events did not result from locomotor activity.

3.4 | Exploration-induced 23–30 Hz power increases predict subsequent performance in the object location test

We next analyzed the 23–30 Hz oscillations in the recall phase, during which time one object was displaced to a novel location while the other object remained in the familiar location (Figure 6a). Similar to

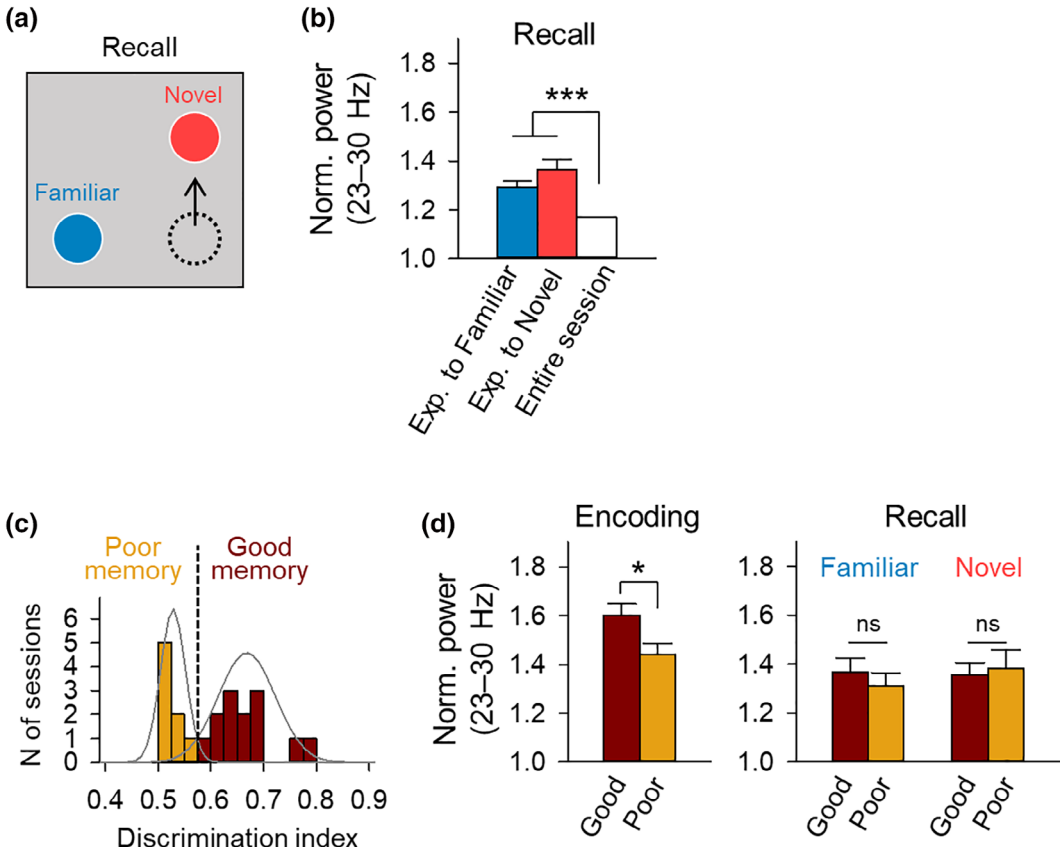

FIGURE 6 Exploration-induced 23–30 Hz power increases predict subsequent performance in the object location test. (a) Experimental diagram of the recall phase. One of the objects was displaced to a *novel* location, whereas the other object remained in the *familiar* location. (b) Mean ± *SEM* exploration-induced 23–30 Hz power before exploring the familiar and novel location objects during the recall was significantly greater than the mean power of the entire session. ***$p < .001$, one-sample *t* test; $n = 79$ and 104 events, respectively, from 21 sessions. (c) All 21 sessions were divided into good memory sessions ($n = 13$) or poor memory sessions ($n = 8$) based on the discrimination indices in the recall phase. Two gray lines indicate the least-square best fit to a bimodal Gaussian distribution. (d) Exploration-induced 23–30 Hz power during the encoding phase (*left*) and the recall phase (*right*) were separately plotted for good and poor memory sessions. $^{ns}p > .05$, *$p < .05$, Student's *t* test; $n = 79$–370 events from 21 sessions [Color figure can be viewed at wileyonlinelibrary.com]

the encoding phase, the 23–30 Hz power was enhanced immediately before the exploration events in the recall phase (Figure 6b; Familiar: $t_{78} = 3.96$, $p = 1.63 \times 10^{-4}$, $n = 79$ events, Novel: $t_{103} = 4.56$, $p = 1.40 \times 10^{-5}$, $n = 104$ events; one-sample *t* test versus the entire session), but there was no significant difference in the 23–30 Hz power between exploration events directed toward the familiar location object and the novel location object (Figure 6b; $t_{182} = 0.187$, $p = .852$, Student's *t* test).

We next examined the relationship of exploration-increased 23–30 Hz powers with task performance. Based on bimodal Gaussian fitting to the discrimination indices, 21 sessions were divided into 13 good memory sessions and 8 poor memory sessions (Figure 6c). In the encoding phase, exploration events in the good memory sessions induced greater increases in the 23–30 Hz power than those in the poor memory sessions (Figure 6d, *left*; $t_{369} = 2.01$, $p = 4.48 \times 10^{-2}$, Student's *t* test; $n = 266$ and 104 events from 21 sessions). This power difference was not observed in the recall phase (Figure 6d, *right*; Familiar: $t_{78} = 0.525$, $p = .601$, $n = 21$–58 events; Novel: $t_{103} = -0.232$, $n = 21$–83 events; $p = .817$, Student's *t* test). These results indicated that greater 23–30 Hz power during exploration events in the encoding phase predicted successful recall of object location memories.

4 | DISCUSSION

In this study, we found that hippocampal beta-band (23–30 Hz) oscillations were transiently enhanced before object exploration in the object location task. Within each session, the exploration-increased 23–30 Hz oscillation power gradually decreased. Greater 23–30 Hz power during memory encoding was linked to better memory recall. Our observations suggest that 23–30 Hz oscillations underlie a neural process for memory acquisition about the location of landmarks.

One of the roles of hippocampal beta oscillations is novelty detection. When animals were placed in a novel environment, the power of 23–30 Hz oscillations in the CA1 region rapidly increased and then gradually decreased as the animals became familiar with the environment (Berke et al., 2008). Hippocampal 23–30 Hz oscillations

were also enhanced during a novel object recognition task (França et al., 2014). This latter study reported that the mean 23–30 Hz power was higher during the memory-encoding phase than during the memory-recall phase, suggesting that the beta oscillation power increased in response to environmental saliency. Interestingly, administration of haloperidol, which acts mainly as a dopamine receptor antagonist, immediately after the encoding phase not only impaired novel object task performance but also inhibited the decrease in 23–30 Hz oscillations during the recall phase (França et al., 2014). These results raised the possibility that hippocampal beta oscillations are modulated by dopaminergic signaling and are potentially usable as a biomarker for novelty perception. Consistent with this idea, dopaminergic signaling in the hippocampus has an important role in novelty-induced enhancement of memory retention (Takeuchi et al., 2016). Therefore, our results indicating that enhanced 23–30 Hz power during memory encoding was correlated with retrieval of object location memories suggest that animals that had successfully perceived objects as "novel" created strong memory traces about the locations of the objects. In other words, novelty detection is accompanied by 23–30 Hz oscillations and contributes to memory acquisition. We believe that hippocampal 23–30 Hz oscillations are a neural candidate for recognizing environmental saliency and determining subsequent memory performance.

Multiple mechanisms are involved in object location memory. A recent study revealed that CA1-projecting subicular neurons support object location memory (Sun et al., 2019). These neurons receive input from the visual cortex and project to the perirhinal cortex. Like the CA1 region, the perirhinal cortex is critical for object memory or novelty recognition (Ho et al., 2015; Nomura et al., 2019), suggesting that the CA1-projecting subicular neurons serve as a hub that links cortical areas (that recognizes objects or their novelty) with the hippocampal structure (that processes spatial information). These neurons also receive dense inputs from CA1 inhibitory neurons. Another study has demonstrated that rhythmic firing of CA1 interneurons with respect to 15–25 Hz oscillations is observed during a context-guided odor-reward association task (Rangel et al., 2016), which suggests that the coordinated firing of CA1 interneurons activates CA1-projecting subicular neurons and facilitates object-location associative learning. This neuronal process may be reflected by beta-frequency local oscillations.

Beta-frequency oscillations have been reported to occur throughout the brain. Learning-dependent enhancement of 15–40 Hz power has been reported in olfactory-associated areas (Chapman, Xu, Haykin, & Racine, 1998; Ravel et al., 2003; Vanderwolf & Zibrowski, 2001). Odor discrimination learning induced olfacto-hippocampal circuit resonance at frequencies of 15–35 Hz (Martin, Beshel, & Kay, 2007). The entorhinal cortex (EC), which integrates multimodal information and provides inputs to the hippocampus, exhibits beta-frequency oscillations. Similar to CA1 neurons (Deshmukh & Knierim, 2013), a subset of medial EC cells encodes positions relative to the object (Høydal, Skytøen, Andersson, Moser, & Moser, 2019), whereas a subpopulation of lateral EC neurons encodes external object locations relative to the animals (Wang et al., 2018). Together, neurons in both medial and lateral EC exhibit object-dependent firing properties. Hippocampal and the lateral EC firing was coordinated at 20–40 Hz during associative learning (Igarashi et al., 2014). Moreover, 15–30 Hz oscillations in the dentate gyrus were suggested to be generated via input from the EC (Rangel, Chiba, & Quinn, 2015). Novelty-induced 23–30 Hz oscillations in the CA1 require NMDA receptor-mediated activity in the CA3 region (Berke et al., 2008). Thus, the EC-dentate-hippocampal circuit may be a source for the generation of 23–30 Hz oscillations. In other words, beta oscillations in the hippocampus may be driven by the EC, which mediates functional coupling between the hippocampus and other brain structures, thereby contributing to object-place associative memory formation.

Moreover, cholinergic signaling modulates hippocampal 23–30 Hz oscillations associated with object location memories. The cholinergic agonist carbachol induced beta oscillations in hippocampal slices (Arai & Natsume, 2006). Object location memories are facilitated by cholinergic agonists or acetylcholine hydrolysis inhibitors, whereas they are impaired by cholinergic antagonists (Assini et al., 2009; Murai et al., 2007). Loss of neurons in the basal forebrain, the major source of cholinergic innervations, has been reported in patients with neuropsychiatric disorders, including Alzheimer's disease (Arendt, Bigl, Arendt, & Tennstedt, 1983). Interestingly, the basal forebrain generates 15–30 Hz oscillations during associative learning (Quinn, Nitz, & Chiba, 2010). Thus, the basal forebrain plays a key role in hippocampal beta oscillations.

Hippocampal oscillations have been associated with respiration or sniffing behavior. Respiration modulates beta-band (10–20 Hz) oscillations in the hippocampus (Lockmann et al., 2018). Although we defined object exploration as sniffing or touching to the objects, we found no evidence showing that exploration-induced 23–30 Hz oscillations were not modulated by sniffing itself. First, sniffing that was not directed to the objects did not induce 23–30 Hz oscillations (Figure 3f). Second, we observed a time-dependent decrease in 23–30 Hz amplitude (Figure 3h), which suggested that 23–30 Hz oscillations were involved in object memory or novelty to the objects but not respiration. Third, exploration-induced beta oscillations (23–30 Hz) had different frequencies than respiration-induced beta oscillations (10–20 Hz).

In conclusion, we found that the hippocampus exhibits 23–30 Hz oscillations immediately before the onset of exploratory behavior toward objects and that these oscillations are associated with better object location memories. Although hippocampal 23–30 Hz oscillations have been known to emerge in novel contexts (Berke et al., 2008; França et al., 2014), our work is the first to link 23–30 Hz oscillations to landmark memories. It remains unclear whether 23–30 Hz oscillations mediate general spatial memory or specific object location memories. Further studies are needed to elucidate how hippocampal 23–30 Hz oscillations contribute to cognitive processes.

ACKNOWLEDGMENTS

This work was supported by JST ERATO (JPMJER1801), JSPS Grants-in-Aid for Scientific Research (18H05525), the Human Frontier Science Program (RGP0019/2016), and the AMED Strategic International Brain Science Research Promotion Program (18dm0307007h0001). This work was conducted partially as a program at the International

Research Center for Neurointelligence (WPI-IRCN) of The University of Tokyo Institutes for Advanced Study at The University of Tokyo. The data that support the findings of this study are available on request from the corresponding author.

DATA AVAILABILITY STATEMENT

The data that support the findings of this study are available from the corresponding author upon reasonable request.

ORCID

Yuji Ikegaya https://orcid.org/0000-0003-2260-8191

REFERENCES

Arai, J., & Natsume, K. (2006). The properties of carbachol-induced beta oscillation in rat hippocampal slices. *Neuroscience Research*, *54*, 95–103.

Arendt, T., Bigl, V., Arendt, A., & Tennstedt, A. (1983). Loss of neurons in the nucleus basalis of Meynert in Alzheimer's disease, paralysis agitans and Korsakoff's disease. *Acta Neuropathologica*, *61*, 101–108.

Assini, F. L., Duzzioni, M., & Takahashi, R. N. (2009). Object location memory in mice: Pharmacological validation and further evidence of hippocampal CA1 participation. *Behavioural Brain Research*, *204*, 206–211.

Barker, G. R., & Warburton, E. C. (2011). When is the hippocampus involved in recognition memory? *The Journal of Neuroscience*, *31*, 10721–10731.

Berke, J. D., Hetrick, V., Breck, J., & Greene, R. W. (2008). Transient 23-30 Hz oscillations in mouse hippocampus during exploration of novel environments. *Hippocampus*, *18*, 519–529.

Buzsáki, G. (2002). Theta oscillations in the hippocampus. *Neuron*, *33*, 325–340.

Buzsáki, G. (2015). Hippocampal sharp wave-ripple: A cognitive biomarker for episodic memory and planning. *Hippocampus*, *25*, 1073–1188.

Buzsáki, G., & Draguhn, A. (2004). Neuronal oscillations in cortical networks. *Science*, *304*, 1926–1929.

Buzsáki, G., & Wang, X. J. (2012). Mechanisms of gamma oscillations. *Annual Review of Neuroscience*, *35*, 203–225.

Chapman, C. A., Xu, Y., Haykin, S., & Racine, R. J. (1998). Beta-frequency (15-35 Hz) electroencephalogram activities elicited by toluene and electrical stimulation in the behaving rat. *Neuroscience*, *86*, 1307–1319.

Colgin, L. L. (2013). Mechanisms and functions of theta rhythms. *Annual Review of Neuroscience*, *36*, 295–312.

Deshmukh, S. S., & Knierim, J. J. (2013). Influence of local objects on hippocampal representations: Landmark vectors and memory. *Hippocampus*, *23*, 253–267.

Ennaceur, A., Neave, N., & Aggleton, J. P. (1997). Spontaneous object recognition and object location memory in rats: The effects of lesions in the cingulate cortices, the medial prefrontal cortex, the cingulum bundle and the fornix. *Experimental Brain Research*, *113*, 509–519.

França, A. S., do Nascimento, G. C., Lopes-dos-Santos, V., Muratori, L., Ribeiro, S., Lobão-Soares, B., & Tort, A. B. (2014). Beta2 oscillations (23-30 Hz) in the mouse hippocampus during novel object recognition. *The European Journal of Neuroscience*, *40*, 3693–3703.

Girardeau, G., Benchenane, K., Wiener, S. I., Buzsáki, G., & Zugaro, M. B. (2009). Selective suppression of hippocampal ripples impairs spatial memory. *Nature Neuroscience*, *12*, 1222–1223.

Ho, J. W., Poeta, D. L., Jacobson, T. K., Zolnik, T. A., Neske, G. T., Connors, B. W., & Burwell, R. D. (2015). Bidirectional modulation of recognition memory. *The Journal of Neuroscience*, *35*, 13323–13335.

Høydal, Ø., Skytøen, E. R., Andersson, S. O., Moser, M. B., & Moser, E. I. (2019). Object-vector coding in the medial entorhinal cortex. *Nature*, *568*, 400–404.

Igarashi, K. M., Lu, L., Colgin, L. L., Moser, M. B., & Moser, E. I. (2014). Coordination of entorhinal-hippocampal ensemble activity during associative learning. *Nature*, *510*, 143–147.

Lockmann, A. L. V., Laplagne, D. A., & Tort, A. B. L. (2018). Olfactory bulb drives respiration-coupled beta oscillations in the rat hippocampus. *The European Journal of Neuroscience*, *48*, 2663–2673.

Martin, C., Beshel, J., & Kay, L. M. (2007). An olfacto-hippocampal network is dynamically involved in odor-discrimination learning. *Journal of Neurophysiology*, *98*, 2196–2205.

Murai, T., Okuda, S., Tanaka, T., & Ohta, H. (2007). Characteristics of object location memory in mice: Behavioral and pharmacological studies. *Physiology & Behavior*, *90*, 116–124.

Nomura, H., Mizuta, H., Norimoto, H., Masuda, F., Miura, Y., Kubo, A., … Ikegaya, Y. (2019). Central histamine boosts perirhinal cortex activity and restores forgotten object memories. *Biological Psychiatry*, *86*, 230–239.

Norimoto, H., Makino, K., Gao, M., Shikano, Y., Okamoto, K., Ishikawa, T., … Ikegaya, Y. (2018). Hippocampal ripples down-regulate synapses. *Science*, *359*, 1524–1527.

Okada, S., Igata, H., Sasaki, T., & Ikegaya, Y. (2017). Spatial representation of hippocampal place cells in a T-maze with an aversive stimulation. *Frontiers in Neural Circuits*, *11*, 101.

Quinn, L. K., Nitz, D. A., & Chiba, A. A. (2010). Learning-dependent dynamics of beta-frequency oscillations in the basal forebrain of rats. *The European Journal of Neuroscience*, *32*, 1507–1515.

Rangel, L. M., Chiba, A. A., & Quinn, L. K. (2015). Theta and beta oscillatory dynamics in the dentate gyrus reveal a shift in network processing state during cue encounters. *Frontiers in Systems Neuroscience*, *9*, 96.

Rangel, L. M., Rueckemann, J. W., Riviere, P. D., Keefe, K. R., Porter, B. S., Heimbuch, I. S., … Eichenbaum, H. (2016). Rhythmic coordination of hippocampal neurons during associative memory processing. *eLife*, *5*, e09849.

Ravel, N., Chabaud, P., Martin, C., Gaveau, V., Hugues, E., Tallon-Baudry, C., … Gervais, R. (2003). Olfactory learning modifies the expression of odour-induced oscillatory responses in the gamma (60-90 Hz) and beta (15-40 Hz) bands in the rat olfactory bulb. *The European Journal of Neuroscience*, *17*, 350–358.

Sun, Y., Jin, S., Lin, X., Chen, L., Qiao, X., Jiang, L., … Xu, X. (2019). CA1-projecting subiculum neurons facilitate object-place learning. *Nature Neuroscience*, *22*, 1857–1870.

Takeuchi, T., Duszkiewicz, A. J., Sonneborn, A., Spooner, P. A., Yamasaki, M., Watanabe, M., … Morris, R. G. (2016). Locus coeruleus and dopaminergic consolidation of everyday memory. *Nature*, *537*, 357–362.

Tort, A. B., Komorowski, R., Eichenbaum, H., & Kopell, N. (2010). Measuring phase-amplitude coupling between neuronal oscillations of different frequencies. *Journal of Neurophysiology*, *104*, 1195–1210.

Tulving, E. (1983). *Elements of episodic memory*. New York: Oxford University Press.

Vanderwolf, C. H., & Zibrowski, E. M. (2001). Pyriform cortex beta-waves: Odor-specific sensitization following repeated olfactory stimulation. *Brain Research*, *892*, 301–308.

Vogel-Ciernia, A., & Wood, M. A. (2014). Examining object location and object recognition memory in mice. *Current Protocols in Neuroscience*, *69*, 1–17.

Wang, C., Chen, X., Lee, H., Deshmukh, S. S., Yoganarasimha, D., Savelli, F., & Knierim, J. J. (2018). Egocentric coding of external items in the lateral entorhinal cortex. *Science*, *362*, 945–949.

How to cite this article: Iwasaki S, Sasaki T, Ikegaya Y. Hippocampal beta oscillations predict mouse object-location associative memory performance. *Hippocampus*. 2021;31: 503–511. https://doi.org/10.1002/hipo.23311